Quantum Electronics **47** (3) 232–235 (2017)

https://doi.org/10.1070/QEL16302

Improvement of hot-electron and gamma-ray yields by selecting preplasma thickness for a target irradiated by a short laser pulse

A.V. Brantov, M.G. Lobok, V.Yu. Bychenkov

Abstract. **The dependences of the temperature and the number of hot electrons on the size of the plasma corona of a thin foil target irradiated by a short relativistically intense laser pulse are investigated by three-dimensional numerical simulations. For a 30-fs long laser pulse with an energy of 300 mJ we have determined the optimal preplasma size which maximises the yield of forward-accelerated electrons capable of generating gamma-ray photons several MeV in energy. A study is made of gamma-ray generation by such laser-accelerated electrons in the bombardment of a converter target placed behind the laser target; the brightness of this gamma-ray source is shown to range up to 10^{15} photons s^{-1} $mrad^{-2}$ mm^{-2} × (0.1 % BW)$^{-1}$.**

Keywords: *gamma-ray radiation, laser pulse of relativistic intensity, three-dimensional simulations.*

1. Introduction

The sources of X-ray radiation that make use of laser methods of electron acceleration have a broad spectrum of potential applications in medicine, biology, materials science and security (inspection) systems [1]. The possibility of employing laser sources has already been demonstrated experimentally for diagnostic radiology involving a phase-contrast imaging technique [2], for inspection relying on high-contrast gamma gamma-ray radiography [3, 4], for the production of medical isotopes via photonuclear reactions in nuclear medicine [5] and for the radiography of high-temperature plasmas [1]. Under broad discussion is the feasibility of employing this X-ray radiation in medicine and biology for three-dimensional pattern reconstruction in the computer tomography with the use of X-ray photons ranging from 15 to 50 keV in energy [6], for radiotherapy and radiosurgery with the use of gamma rays [7]. In the latter case we are dealing with the replacement of the traditional cobalt 60 isotope gamma-ray source, which emits gamma-ray photons with energies of 1.17 and 1.33 MeV.

A.V. Brantov, V.Yu. Bychenkov P.N. Lebedev Physics Institute, Russian Academy of Sciences, Leninsky prosp. 53, 119991 Moscow, Russia; Centre for Fundamental and Applied Research, N.L. Dukhov All-Russia Research Institute of Automatics (VNIIA), 'Rosatom', Sushchevskaya ul. 22, 127055 Moscow, Russia;
e-mail: brantov@sci.lebedev.ru, bychenk@sci.lebedev.ru;
M.G. Lobok Centre for Fundamental and Applied Research, N.L. Dukhov All-Russia Research Institute of Automatics (VNIIA), 'Rosatom', Sushchevskaya ul. 22, 127055 Moscow, Russia

Received 6 February 2017
Kvantovaya Elektronika **47** (3) 232–235 (2017)
Translated by E.N. Ragozin

This work is a continuation of our previous investigations in the optimisation of laser-plasma targets irradiated by a femtosecond laser pulse for the purpose of efficient electron acceleration and production of secondary radiation in the X- and gamma-ray frequency ranges [8]. The preplasma (corona) size is the determinative parameter for the production of as large as possible a number of laser-accelerated electrons with an energy of several MeV and maximising the hard X-ray yield. Previously, we showed how lengthening the preplasma improved the yield of gamma-ray photons with energies below 1 MeV from the converter target irradiated by laser-accelerated electrons [8], but the optimal preplasma size was not determined. In the present work we continue lengthening the preplasma and find its optimal size, discuss the effect of preplasma profile on the electron acceleration, and analyse in detail the secondary hard radiation spectra produced by the action of a laser-accelerated electron beam on different converter targets.

2. Electron acceleration from targets with a lengthy plasma corona

The main task of our simulations was the search for the optimal layered target intended for a high-efficiency generation of an electron beam which penetrates through the target irradiated by a laser beam of relativistic intensity. We study the electron generation from a foil with a preplasma, or plasma corona, which may be produced at the front target surface, because the laser pulse is preceded by a rather long, commonly nanosecond-long, prepulse or by a shorter laser pulse of higher intensity. The employment of both versions permits controlling the resultant corona parameters. Mention should be made of Ref. [9] dedicated to the diagnostics of a preliminarily produced preplasma, which permits exerting effect on the corona parameters by controlling the prepulse intensity and delay, the target composition, etc.

The simulation of laser radiation–plasma interaction was performed using the three-dimensional, fully relativistic particle-in-cell Mandor code [10]. In these three-dimensional simulations, a linearly polarised 30-fs long laser pulse with a Gaussian temporal intensity distribution was focused onto the front target surface to a 4-μm diameter focal spot with a Gaussian radial intensity distribution. The peak laser radiation intensity 5 × 10^{19} W cm^{-1} (which corresponds to the dimensionless laser field amplitude $a_0 = 6$ for a wavelength $\lambda = 1$ μm) corresponded to a laser pulse energy of 0.3 J. In all calculations we considered the normal incidence of the laser pulse onto a target composed of electrons of mass m_e and of heavy ions of charge Z and mass m_i ($Zm_e/m_i = 1/3672$), the electron density being equal to 100 times the critical density.

The preplasma was modelled with a linearly increasing profile of the electron density, which grew from zero to the critical electron density n_c over a length varied in our simulations from 10 to 60 μm. The thickness of the principal target was equal to 0.05 μm. Along with the linear profile, we also considered an exponential preplasma profile, $n_e = 2n_c\exp(-x/L)$, where L = 5 μm for a preplasma thickness of 20 μm and 10 μm for a preplasma thickness of 40 μm.

In our three-dimensional simulations, use was made of a spatial grid step $x \times y \times z = 0.02 \times 0.05 \times 0.05$ μm, where x (the longitudinal direction) corresponds to the propagation direction of a laser pulse polarised in the z-direction. The entire simulation domain dimension was equal to 20 μm in both transverse directions and was varied from 60 to 100 μm in the longitudinal direction, depending on the preplasma size. Recorded in the simulations was the spectrum of electrons escaping into a cone opening angle of 90° behind the target.

The simulation results of electron acceleration from targets with different linear preplasma profiles are shown in Fig. 1. One can clearly see that a preplasma length of 20 μm corresponds to the generation of practically the maximum number of high-energy electrons. Increasing the preplasma length to 40 μm results only in an insignificant growth of the number and energy of the highest-energy particles. The further preplasma lengthening does not entail a gain in energy and number of accelerated electrons, which is due to depletion of the laser pulse. Therefore, the preplasma with a characteristic thickness of 20–40 μm is optimal for the electron acceleration by a femtosecond laser pulse with an energy of 300 mJ. The spectrum of accelerated electrons, strictly speaking, is not a Maxwellian spectrum with a single temperature. However, as is evident from Fig. 1, the average accelerated electron energy (temperature) lies between 5 and 7 MeV. The total charge of the beam of electrons ejected behind the target is equal to ~1 nC and its characteristic transverse size is equal to ~10 μm. We note that the preplasma profile has only a slight effect on the efficiency of particle acceleration. In particular, it is possible to select an exponential density profile (Fig. 2) which provides virtually the same number of hot electrons as a linear profile. The highest-energy electrons (40 MeV or above) fly in the direction of laser beam propagation into an angle $\theta \leqslant 10°$ (Fig. 3), while the bulk of above-10 MeV electrons are rather poorly collimated ($\theta \leqslant 40°$).

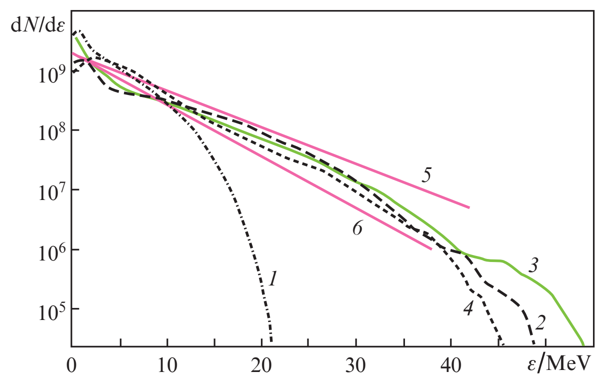

Figure 1. Spectra of electrons ejected into a cone opening angle of 90° behind the target by the instant of simulation termination (t = 320 fs) in the irradiation of a 0.05-μm thick target with a preplasma with a linear density profile varying from zero to the critical density over a preplasma length of (*1*) 10, (*2*) 20, (*3*) 40 and (*4*) 60 μm. The straight lines correspond to Maxwellian distributions with temperatures of (*5*) 7 and (*6*) 5 MeV.

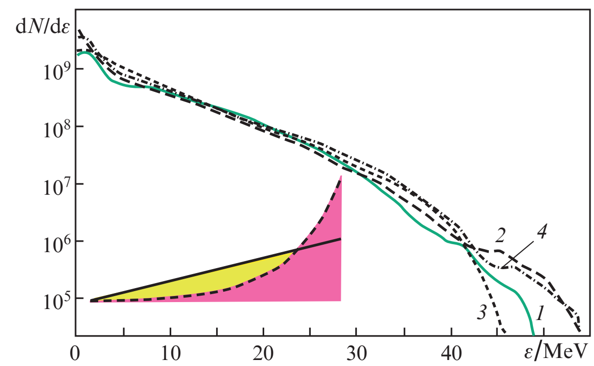

Figure 2. Comparison of the spectra of electrons ejected behind the target in the irradiation of the target (0.05 μm) with a preplasma with a linear density profile (*1*, *2*) and a preplasma with an exponential profile (*3*, *4*), with the preplasma density varying from zero to the critical density over a length of (*1*, *3*) 20 and (*2*, *4*) 40 μm.

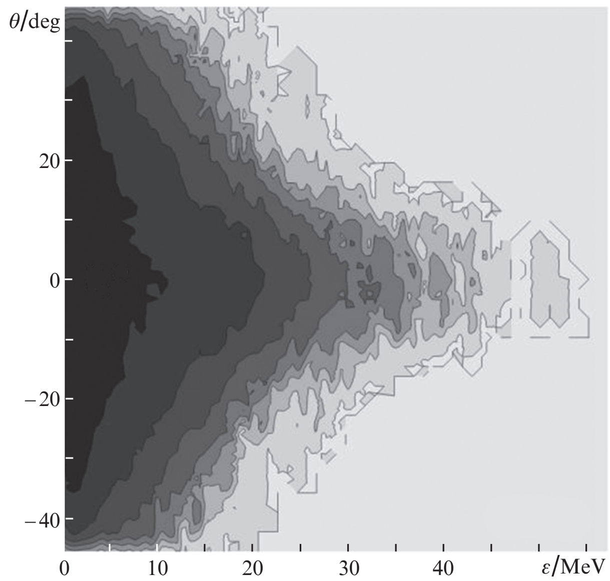

Figure 3. Angular distribution of the electrons ejected behind the target in the irradiation of the target with a preplasma with a linear density profile varying from zero to the critical density over a length of 20 μm. Each contour corresponds to about a five-fold decrease in electron concentration.

As noted in our previous work [8], the electron acceleration in a corona takes place due to stochastic heating in complex laser-plasma fields, which is caused by the emergence of a standing laser field, a longitudinal electric field, and the radial electric field in the plasma channel of the preplasma, as well as by the development of plasma instabilities.

3. Use of accelerated electron beams for generating gamma-ray radiation

The electron beams accelerated by a short laser pulse were used for calculating the production of gamma-rays from the second target (converter target) placed immediately behind the laser target. We note that the bremsstrahlung generation of hard radiation in the corona is heavily suppressed because of the low preplasma density and the low ion charge. The possible collisionless production of hard photons by betatron radiation [11, 12], which in principle may be significant for a rather lengthy corona, is insignificant in the case under consideration owing to the relatively small preplasma size.

To analyse the generated gamma-ray radiation, the electrons accelerated in the laser target, which were obtained by the three-dimensional simulation with the Mandor code, were employed as input to the GEANT-4 code. The function of the converter was fulfilled by tantalum, gold and copper foils 400 μm and 2 mm in thickness. Our calculations served to numerically record the gamma-ray radiation transmitted through the converter as well as backward propagating gamma-rays (in front of the converter). In addition, we recorded the transmitted electron flux.

The spectra of the secondary radiation transmitted through the target are depicted in Fig. 4 for all kinds of converter targets of thickness 2 mm. All characteristic lines of the metals are readily seen in the low-energy part of the spectrum (see the inset in Fig. 4). The 'temperature' of gamma-ray radiation caused by the bremsstrahlung is independent of the converter target and amounts to 4 MeV in our case. At the same time, the number of high-energy photons rises with the atomic number of the converter; for gold and tantalum it turns out to be higher by about an order of magnitude than for copper. It is possible to estimate the total energy of gamma-ray radiation transmitted through the converter target. For the gold target it amounts to 14.3 μJ, which corresponds to a laser-to-gamma-ray energy conversion coefficient of $\sim 5 \times 10^{-5}$. The use of a copper target lowers the X-ray radiation energy to 7 μJ.

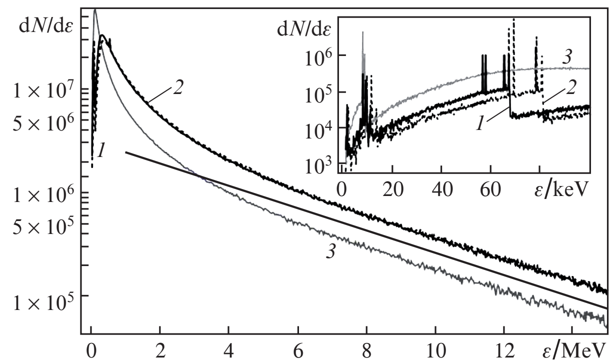

Figure 4. Spectra of X-ray radiation from converter targets made of (*1*) tantalum, (*2*) gold and (*3*) copper irradiated by the electrons which are accelerated from the target with a preplasma of length 20 μm. The converter target thickness was equal to 2 mm. The straight line is the exponential spectrum for a temperature of 4 MeV. The inset shows the low-energy domain, which exhibits the lines corresponding to the characteristic radiation.

Figure 5 shows the dependence of the gamma-ray radiation spectrum on the thickness of the gold converter target. Thinning the target to 400 μm results in a lowering of the total gamma-ray radiation energy to 11 μJ. In this case, the spectral power density in the low-energy part of the spectrum and the intensity of the characteristic radiation lines become somewhat higher. At the same time, the characteristic radiation turns out to be even stronger for the backward gamma-ray radiation from the converter, in whose spectrum the bremsstrahlung radiation is heavily suppressed (see the curves in Fig. 5). We emphasise that the low-energy part of the spectrum (below 100 keV), which comprises the characteristic radiation, accounts for an energy of no more than 0.1 μJ. The pulse duration of the X-ray source depends on the converter target thickness [13] and amounts to about 7 ps for the 2-mm thick target; for the target of thickness 400-μm it amounts to only 1.5 ps.

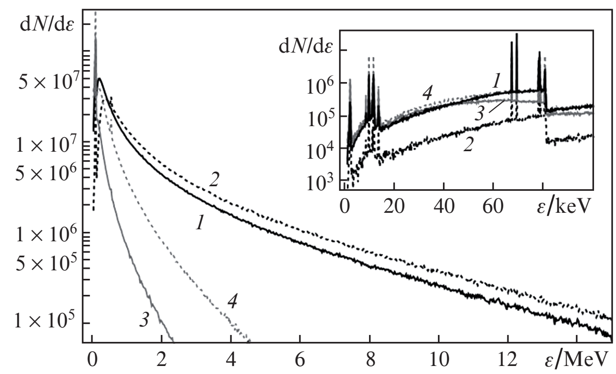

Figure 5. Spectra of (*1*, *2*) transmitted and (*3*, *4*) reflected X-ray radiation from the gold converter target of thickness (*2*, *4*) 2 mm and (*1*, *3*) 400 μm irradiated by the electrons which are accelerated from the target with a preplasma of size 20 μm. The inset shows the low-energy domain of the hard X-ray spectrum with the lines corresponding to the characteristic radiation.

The angular distribution of the secondary radiation depends on the photon energy. In the energy domain of about several MeV it amounts to $\sim 10°$. The source coincides in size with the electron beam, provided the converter target is located immediately behind the laser target. This permits estimating the gamma-ray source brightness, which amounts to about 10^{15} photons s^{-1} $mrad^{-2}$ mm^{-2} $(0.1\,\%\,BW)^{-1}$ at a gamma-ray photon energy of 0.5–1.5 MeV. As the photon energy increases to 5 MeV, the source brightness lowers by about two-fold. We note that the use of a thinner converter target provides, despite a decrease in the total number of 1-MeV photons by 20 %–30 %, a higher source brightness due to a shortening of the source duration.

To estimate the efficiency of energy transfer from the incident electron beam, the spectra of electrons transmitted through the converter target are shown in Fig. 6. One can

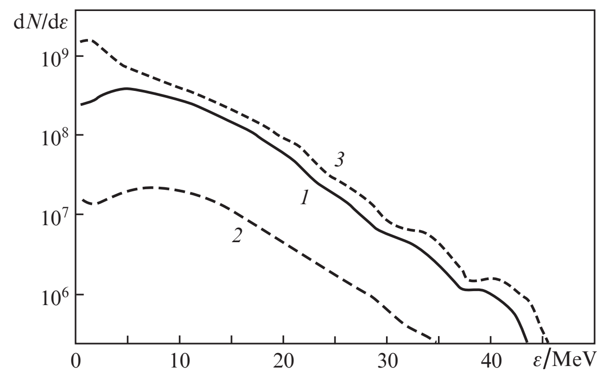

Figure 6. Spectra of the electrons transmitted through targets of thickness (*1*) 400 μm and (*2*) 2 mm as well as (*3*) incident electron beam spectrum.

clearly see that a large fraction of the hot electrons, which account for approximately 60% of the incident beam energy, are transmitted through the 400-μm thick target. Thickening the target to 2 mm results in a significant decrease in the number of transmitted electrons and their energy: the transmitted beam accounts for only 4% of the incident beam energy. Therefore, a further increase in target thickness would not entail an appreciable growth of gamma-ray generation efficiency.

4. Conclusions

With the help of three-dimensional numerical simulations we determined the optimal preplasma size for the efficient electron acceleration by a femtosecond laser pulse with an energy of 300 mJ. By optimising the electron acceleration from a target with a preplasma, as shown here, it is possible to significantly increase the number of accelerated electrons and their energy, thereby improving the laser-to-gamma-ray energy conversion efficiency by a factor of five in comparison with the previously studied case of electron acceleration in the preplasma whose length was different from the optimal one determined here [8]. (We emphasise that an error was made in Ref. [8] as regards the total number of hard X-ray photons generated: instead of 4×10^9 one should read 2×10^7 X-ray photons with energies ranging from 0.1 to 2 MeV.)

Our simulations with the optimal target predict the generation of 4×10^7 gamma-ray photons with energies ranging from 0.1 to 15 MeV and a temperature of ~4 MeV. Assuming the laser operation at a kilohertz repetition rate, this source may be employed for the radiography of dense static objects with penetration to a depth of several centimetres. In this case, the source brightness peaks in the ~1 MeV energy domain in the forward direction and amounts to 10^{15} photons s^{-1} $mrad^{-2}$ mm^{-2} $(0.1\%\ BW)^{-1}$. Consequently, for a laser with a pulse energy of 30 J one might expect a brightness comparable with the brightness of third-generation synchrotrons at a gamma-ray energy of ~1 MeV.

Acknowledgements. This work was supported by the Presidium of the Russian Academy of Sciences (Programme 'Extreme laser radiation: physics and fundamental applications') and the Russian Foundation for Basic Research (Grant Nos 14-29-09244-ofi-m, 15-02-03042-a and 16-02-00088-a).

References

1. Albert F., Thomas A.G.R. *Plasma Phys. Control. Fusion*, **58**, 103001 (2016).
2. Wenz J., Schleede S., Khrennikov K., Bech M., Thibault P., Heigoldt M., Pfeiffer F., Karsch S. *Nat. Commun.*, **6**, 7568 (2015).
3. Courtois C. et al. *Phys. Plasmas*, **20**, 083114 (2013).
4. Brenner C.M., Mirfayzi S.R., Rusby D.R., et al. *Plasma Phys. Control. Fusion*, **58**, 014039 (2016).
5. Reed S.A. et al. *Appl. Phys. Lett.*, **89**, 231107 (2006).
6. Cole J.M., Wood J.C., Lopes N.C., et al. *Sci. Rep.*, **5** 13244 (2015).
7. Weeks K.J., Litvinenko V.N., Madey J.M.J. *Med. Phys.*, **24**, 417 (1997); Girolami B., Larsson B., Preger M., Schaerf C., Stepanek J. *Phys. Med. Biol.*, **41**, 1581 (1996).
8. Brantov A.V., Lobok M.G., Bychenkov V.Yu. *Quantum Electron.*, **46** (4), 342 (2016) [*Kvantovaya Elektron.*, **46** (4), 342 (2016)].
9. Krestovskikh D.A., Ivanov K.A., Tsymbalov I.N., Shulyapov S.A., Bukin V.V., Volkov R.V., Rupasov A.A., Savel'ev A.B. *Quantum Electron.*, **47** (1), 42 (2017) [*Kvantovaya Elektron.*, **47** (1), 42 (2017)].
10. Romanov D.V., Bychenkov V.Yu., Rozmus W., Capjack C.E., Fedosejevs R. *Phys. Rev. Lett.*, **93**, 215004 (2004).
11. Esarey E., Shadwick B.A., Catravas P., Leemans W.P. *Phys. Rev. E*, **65**, 056505 (2002).
12. Kiselev S., Pukhov A., Kostyukov I. *Phys. Rev. Lett.*, **93**, 135004 (2004).
13. Cipiccia S., Wiggins S.M., Shanks R.P., et al. *J. Appl. Phys.*, **111**, 063302 (2012).